Metallophysics and Advanced Technologies
Металофіз. новітні технол.
Metallofiz. Noveishie Tekhnol.
2026, vol. 48, No. 5, pp. 537–548
https://doi.org/10.15407/mfint.48.05.0537
Reprints available directly from the publisher

PACS numbers: 06.60.Vz, 46.55.+d, 61.72.Ff, 62.20.Qp, 68.47.De, 81.20.Vj, 81.40.Pq

Wear Behaviour of AA 7075 Joints Made by Double-Side Friction Stir Welding

V. Kiran Kumar[*,**], K. V. Durga Rajesh[*], S. R. Koteswara Rao[***], P. Venkateswara Babu[**], T. Srinivasa Rao[****]

[*]*Department of Mechanical Engineering,*
Koneru Lakshmaiah Education Foundation,
522 302 Vaddeswaram,
Andhra Pradesh, India
[**]*Department of Mechanical Engineering,*
Vasireddy Venkatadri Institute of Technology,
522 508 Nambur,
Guntur, Andhra Pradesh, India
[***]*Department of Mechanical Engineering,*
Sri Sivasubramaniya Nadar College of Engineering,
603 110 Chennai,
Tamil Nadu, India
[****]*Cornerstone Academy Private Limited,*
600 129 Chennai,
Tamil Nadu, India

Friction stir welding (FSW) of aluminium alloys became increasingly important across many industries, where the welded joints are required to have acceptable structural and functional properties. Conventional single-side FSW (SS-FSW), particularly, in thick-section joints, leads frequently to a reduction in weld properties, because of excessive heat input. Double-side friction stir welding (DS-FSW) has arisen as a potential solution to mitigate these limitations by balancing the thermal cycles and improving joint properties. In the present work, DS-FSW is executed on AA7075-T651 10 mm thick

Corresponding author: V. Kiran Kumar
E-mail: kiran.rlwc@gmail.com

Citation: V. Kiran Kumar, K. V. Durga Rajesh, S. R. Koteswara Rao, P. Venkateswara Babu, and T. Srinivasa Rao, Wear Behaviour of AA 7075 Joints Made by Double-Side Friction Stir Welding, *Metallofiz. Noveishie Tekhnol.*, **48**, No. 5: 537–548 (2026), DOI: 10.15407/mfint.48.05.0537

plates, and the resulting joints are evaluated methodically for wear performance with the help of a pin-on-disc wear testing setup. The microstructural features and precipitate morphology are also evaluated through optical microscopy and transmission electron microscopy. The DS-FSW joints exhibit superior wear performance, as evidenced by lesser friction coefficients and reduced specific wear rates, in comparison with both the base material and SS-FSW joints. Metallurgical characterization shows that the weld nugget of DS-FSW contained fine equiaxed grains, accompanied by significant reprecipitation of strengthening phases following their dissolution during welding. The combined effects of grain refinements and enhanced retaining of hardening precipitates are identified as the primary contributors to the improved wear resistance of DS-FSW joints. Overall, the findings establish DS-FSW as an effective technique for improving the wear properties of high-strength aluminium-alloy welds, chiefly in thick-section applications.

Key words: double-side friction stir welding, AA 7075, wear behaviour, optical microscopy, transmission electron microscopy.

Зварювання тертям з перемішуванням (ЗПТ) алюмінійових стопів стає все більш важливим у багатьох галузях промисловости, де від зварних з'єднань вимагаються прийнятні структурні та функціональні властивості. Традиційне одностороннє ЗПТ, особливо в товстоперерізних з'єднаннях, часто призводить до пониження властивостей зварного шва через надмірне підведення тепла. Двостороннє зварювання тертям з перемішуванням виникло як потенційне рішення для пом'якшення цих обмежень шляхом балансування термічних циклів і поліпшення властивостей з'єднань. У даній роботі двостороннє зварювання тертям з перемішуванням було виконано на пластинах AA7075-T651 товщиною у 10 мм, а одержані з'єднання були методично оцінені на зносостійкість за допомогою установки для випробування на знос «штифт на диску». Мікроструктурні особливості та морфологія преципітатів також були оцінені за допомогою оптичної мікроскопії та просвітлювальної електронної мікроскопії. З'єднання продемонстрували чудову зносостійкість, про що свідчать менші коефіцієнти тертя та понижені питомі швидкості зносу порівняно як з основним матеріялом, так і з'єднаннями одностороннім ЗПТ. Металурґійна характеризація показала, що заготівка, зварювана двостороннім ЗПТ, містила дрібні рівновісні зерна, що супроводжувалося значним повторним осадженням зміцнювальних фаз після розчинення їх під час зварювання. Сукупний вплив подрібнення зерен і поліпшеного вмісту зміцнювальних осадів визначено як основні чинники, що сприяють поліпшенню зносостійкости з'єднань двостороннім ЗПТ. Загалом, одержані результати визначають двостороннє ЗПТ як ефективну техніку для поліпшення зносостійкости зварних швів високоміцних алюмінійових стопів, головним чином, у товстопрофільних застосуваннях.

Ключові слова: двостороннє зварювання тертям з перемішуванням, стоп AA 7075, зношування, оптична мікроскопія, просвітлювальна електронна мікроскопія.

(Received 31 August, 2025; in final version, 1 May, 2026)

1. INTRODUCTION

7000 series aluminium alloys, particularly, AA7075, are widely employed in automotive, aerospace, and structural sectors owing to their superior strength to weight ratios. However, their weldability is limited with conventional fusion techniques due to solidification cracking and strength degradation. Friction stir welding (FSW), a solid-state welding, has emerged as an effective alternative, with extensive studies addressing weld formation mechanisms, microstructural evolution, mechanical behaviour [1–3], and the influence of tool design [4–8] and process modelling [9, 10]. Advanced variants like friction stir additive manufacturing (FSAM) and friction stir processing (FSP) have further expanded applications in microstructural refinement, composite fabrication, and solid-state manufacturing [11–14].

Most FSW research has focused on plates below 10 mm thickness, while studies on thick sections highlight challenges in thermal management and joint performance [15–19]. Double-sided FSW, involving sequential welding from both sides, has been proposed to overcome these limitations by improving heat distribution and microstructural uniformity [20–22]. Although DS-FSW has shown promise in enhancing the mechanical performance of thick-section joints [23–26], limited work has explored its influence on wear properties of AA7075. To address this gap, the present study investigates DS-FSW of 10 mm thick AA7075 plates with emphasis on wear behaviour.

2. EXPERIMENTAL PROCEDURES

In this work, 10 mm thick rolled AA7075-T651 plates (110 mm × 250 mm) were used as the base material. The alloy composition [wt.%] was as follows: 6.00 Zn, 2.50 Mg, 1.40 Cu, 0.20 Cr, 0.08 Fe, 0.05 Ti, 0.03 Si, 0.01 Mn, with remaining Al. Double-side friction stir welds were produced sequentially, with the second pass executed such that the advancing side of Side *1* corresponded to the retreating side of Side *2*, ensuring balanced material flow and heat distribution. For comparison, single-side welds were also prepared. Welding parameters and tool designs were adopted from previous studies by the present authors [17, 23], with a constant tool tilt angle of 2° for both processes. Representative images of tools and welded plates are shown in Figs. 1 and 2.

Metallographic characterization was performed using optical microscopy and transmission electron microscopy (TEM). Specimens were extracted from heat-affected zone (HAZ), thermomechanically affected zone (TMAZ), weld nugget (WN) and base material (BM). Standard metallographic preparation included grinding with SiC papers, polishing with diamond suspension, and etching in Keller's reagent. Microstructural features were recorded at various magnifications using an

Fig. 1. Images of FSW tool: *a*—DS-FSW, *b*—SS-FSW.

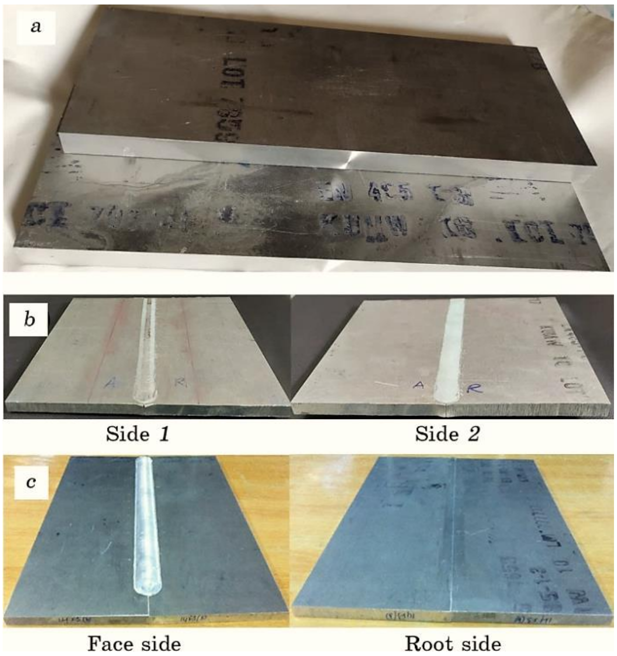

Fig. 2. Photographs of AA7075 plates before and after joining: *a*—As-received plates, *b*—DS- FSW, *c*—SS-FSW.

Olympus optical microscope.

Transmission electron microscopy was employed to examine precipitate morphology across different weld zones. Specimens were sectioned using an electrical discharge machine to minimize mechanical damage, followed by slow manual thinning to avoid thermal effects. Final thinning was performed electrolytically in a nitric acid–methanol solution to obtain electron-transparent foils. TEM observations were carried out using a JEM-2100 microscope.

Wear tests were performed using a pin-on-disc apparatus (Fig. 3) under dry sliding conditions following ASTM G99 standards. The set-up comprises a controller, testing unit and display unit. In the testing unit, a lever mechanism applied normal load to the stationary pin against the rotating disc, with the pin firmly held in a pin holder. Linear variable differential transducer (LVDT) sensors measured friction force and wear displacement, enabling calculation of the wear rate and friction coefficient. The controller unit regulated disc speed to maintain accurate sliding conditions.

Pin samples (10 mm×10 mm cross-section) were extracted from the weld nugget region (Fig. 4). The counter face disc was EN31 steel, 8 mm thick and 80 mm in diameter. Both pin and disc were ultrasonically cleaned in acetone for 10 min prior to testing. The pin was mounted vertically in the holder, and a normal load was applied against the rotating disc at the prescribed speed and sliding distance/time. Real-time friction force, friction coefficient, and wear displacement were recorded during testing. The test parameters considered for the work are provided in Table 1. The experiments were conducted on BM, SS-FSW and DS-FSW pin samples against the EN 31 rotating disc.

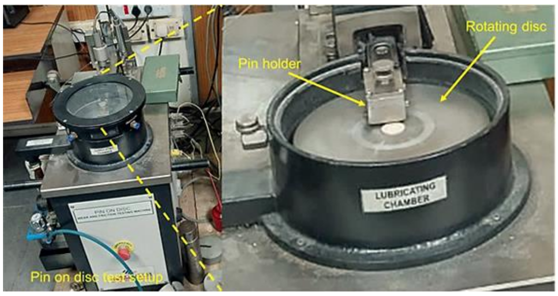

Fig. 3. Images of FSW tool: *a*—DS-FSW, *b*—SS-FSW

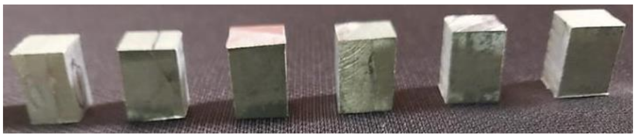

Fig. 4. Pin samples for tribological testing.

TABLE 1. Test parameters.

Parameter	Value	Unit
Normal load (F_n)	60, 80, 100	N
Speed (N)	500, 600, 700	rpm
Sliding time (t)	180	sec
Stationary pin roughness (R_a for pin)	0.31	microns
Rotating disc roughness (R_a for disc)	0.28	microns

All experiments were carried out for a constant duration of 180 seconds across different load–speed combinations. Each test was repeated three times, and the average values of specific wear rate and friction coefficient were considered. The weight of each pin was measured before and after testing, and weight loss was used to calculate the specific wear rate. Tribological parameters, namely friction coefficient and specific wear rate (SWR) [$mm^3/(N \cdot m)$], were determined using the following equations:

$$\text{friction coefficient} = F_f/F_n \ ; \ \text{specific wear rate} = (W_i - W_f)/(\rho F_n S) \ .$$

Here, F_f = force of friction [in N], F_n = normal load [in N], W_i = weight of the pin sample before the experiment [in g], W_f = weight of the sample after the experiment [in g], ρ = density of the pin material [in g/mm^3], and S = sliding distance [in m].

3. RESULTS AND DISCUSSION

3.1. Friction Coefficient

Figure 5 illustrates the effect of normal load and rotational speed on the friction coefficient. At 500 rpm, the coefficient increased with load due to higher interfacial pressure and ploughing action. Among all conditions, BM exhibited the highest friction coefficient, while DS-FSW showed the lowest, indicating superior resistance to sliding. With increasing rotational speed, the coefficient decreased for all samples; however, BM remained more sensitive to speed, particularly at lower ranges. DS-FSW consistently demonstrated a substantial reduction in friction coefficient, especially at higher speeds, suggesting smoother sliding with reduced asperity contact.

3.2. Specific Wear Rate

The influence of normal load and speed on specific wear rate is shown

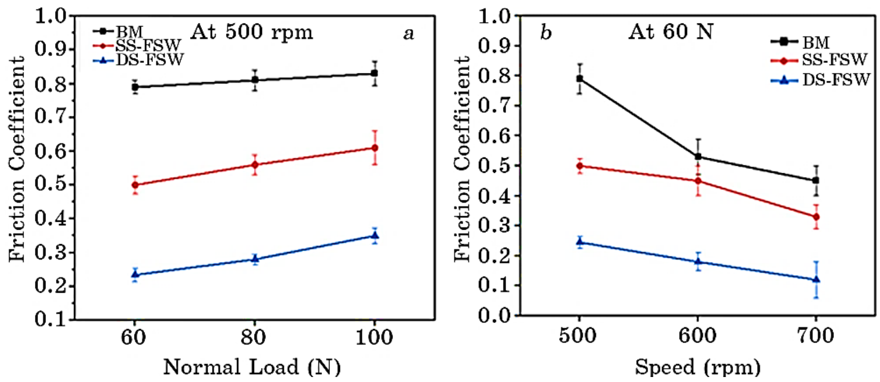

Fig. 5. Variation in friction coefficient with normal load and speed: *a*—normal load, *b*—speed.

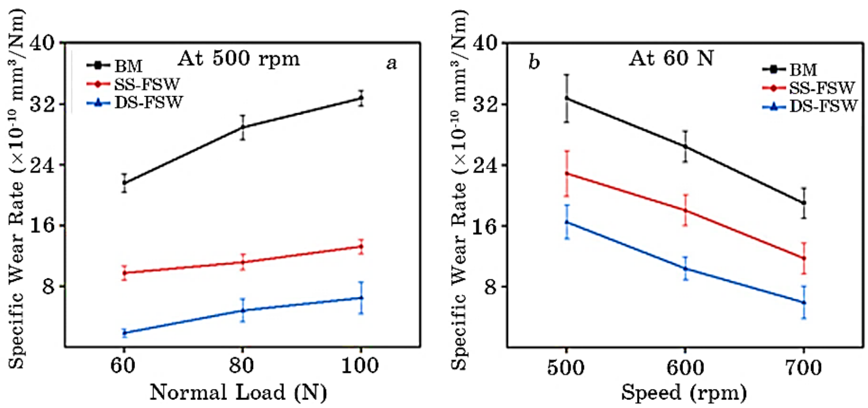

Fig. 6. Variation in specific wear rate with normal load and speed: *a*—normal load, *b*—speed.

in Fig. 6. BM again exhibited the highest SWR across all conditions, with a sharp rise at higher loads due to severe plastic deformation and material removal. DS-FSW samples demonstrated the lowest SWR, attributable to smoother and work-hardened surfaces coupled with lower interfacial shear stresses. With increasing rotational speed (500–700 rpm), SWR decreased for all samples, because higher speeds generally favoured reduced abrasive contact resulting in comparatively lower SWR.

Overall, DS-FSW joints exhibited superior tribological performance, simultaneously reducing both the friction coefficient and SWR compared to BM and SS-FSW samples. The combination of fine-grained microstructure and higher survival of strengthening precipitates likely contributed to their enhanced wear resistance. Favourable

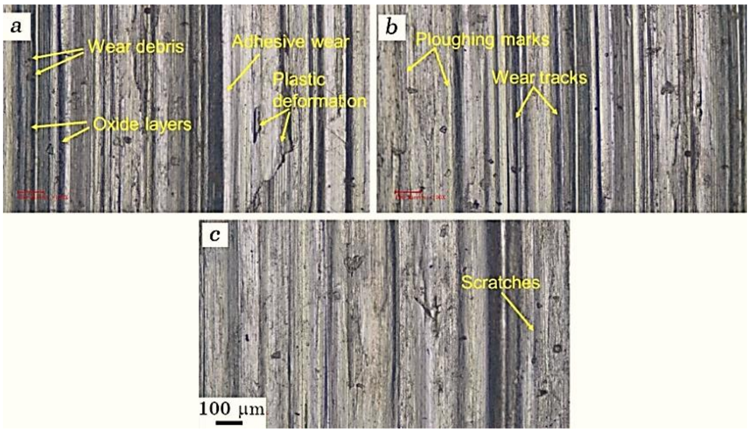

Fig. 7. The worn surfaces of pin samples at a load of 100 N and speed of 500 rpm: *a*—BM, *b*—SS-FSW, and *c*—DS-FSW.

tribological conditions were achieved under lower loads and higher speeds, where DS-FSW joints maintained stable friction and minimized material loss.

3.3. Surface Analysis

Typical worn surface micrographs of BM, SS-FSW, and DS-FSW samples are shown in Fig. 7.

Abrasive wear is evident through scratches, ploughing marks, and plastic deformation along the sliding direction, further aggravated by wear debris acting as third-body particles. Smooth smeared regions indicate adhesive wear, while dark oxide layers suggest oxidative wear due to frictional heating. These mechanisms were observed in all samples tested at 100 N load and 500 rpm. However, DS-FSW samples showed fewer grooves and lower weight loss, demonstrating reduced wear severity, consistent with their minimum specific wear rate values presented in Fig. 6.

3.4 Optical Microscopy

Representative micrographs of the base material and weld zones are given in Fig. 8. The base metal showed large, elongated pancake shaped grains (Fig. 8, *a*), typical of hot-rolled 7000 series alloys. In contrast, the weld nugget displayed fine equiaxed grains (Fig. 8, *b*), confirming extensive dynamic recrystallization brought by frictional heating and severe plastic deformation during FSW, in agreement with earlier reports [17, 18]. Grain refinement in the nugget zone is a key factor con-

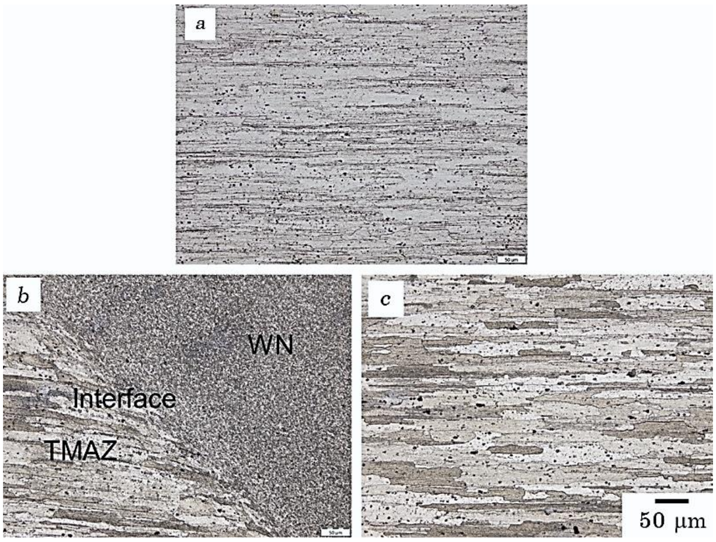

Fig. 8. Typical microstructures: *a*—base material, *b*—WN–TMAZ interface, and *c*—HAZ.

tributing to the reduced wear rate of the welded joints compared with the base material.

The thermo-mechanically affected zone represents the transition between the weld nugget and the heat-affected zone. In this region, the tool induces elevated temperatures and partial plastic deformation, resulting in elongated grains without recrystallization (Fig. 8, *b*). Alongside the TMAZ, the HAZ experiences only thermal exposure, leading to limited grain coarsening as shown in Fig. 8, *c*.

3.5. Transmission Electron Microscopy

Figure 9 illustrates the precipitate morphology of AA7075 in the T651 condition and within the TMAZ and HAZ. The base metal (Fig. 9, *a*) exhibited two distinct classes of strengthening precipitates, consistent with reports by Wert [27] and Lorimer [28]. Larger precipitates (40–60 nm) were identified either as $Mg(Zn_2, AlCu)$ or $Mg_{32}(Al, Zn)_{49}$ phases, while smaller precipitates (10–15 nm) contributed significantly to the alloy high strength. Precipitation hardening achieved through deformation and artificial aging in the T651 temper conditions for the alloy ultimate tensile strength of ≅600 MPa, compared with ≅200 MPa in the annealed state.

The TEM micrograph of the TMAZ (Fig. 9, *b*) revealed partial dissolution of precipitates. While the larger particles remained largely unaffected, the finer precipitates showed slight coarsening. In the HAZ

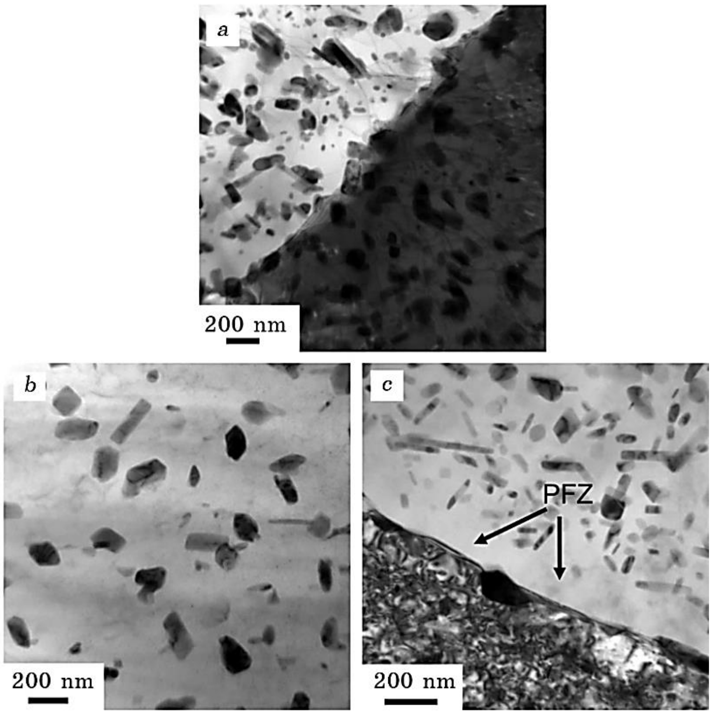

Fig. 9. Typical TEM images showing precipitate morphology in *a*—base material, *b*—TMAZ, and *c*—HAZ.

(Fig. 9, *c*), precipitates were uniformly distributed within grains, but precipitate-free zones (PFZs) were evident along grain boundaries. PFZ formation, widely reported in heat-treated AA7075 alloys, results from dissolution of boundary-adjacent precipitates during heating and their preferential re-precipitation along grain boundaries upon cooling.

TEM images of the weld nugget for SS-FSW and DS-FSW joints are shown in Fig. 10. The thermal cycles during FSW, typically above the solutionizing temperature but below the melting point, caused dissolution of strengthening precipitates, followed by partial re-precipitation and coarsening (Fig. 10, *a*). In DS-FSW joint (Fig. 10, *b*), a higher density and slightly larger size of precipitates were observed compared with SS-FSW, likely due to more favourable thermal conditions. The greater retention of hardening precipitates in DS-FSW explains its superior wear resistance.

4. CONCLUSIONS

1. AA7075–T651 aluminium alloy plates (10 mm thick) were success-

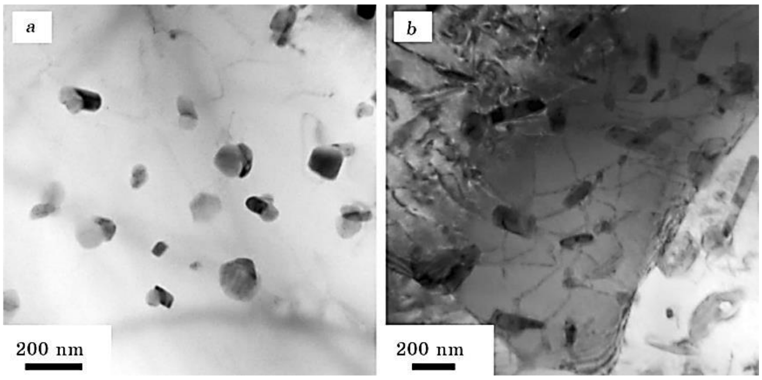

Fig. 10. Transmission electron micrographs of the WN: *a*—SS-FSW *b*—DS-FSW.

fully joined using single-side and double-side friction stir welding, and their wear performance was systematically evaluated.

2. DS-FSW joints exhibited superior wear resistance, reflected in lesser friction coefficients and specific wear rates than both the base material and SS-FSW joints. This improvement is attributed to dynamic recrystallization and enhanced retention of hardening precipitates in the weld nugget.
3. Friction coefficient and specific wear rate improved with applied normal load but decreased with sliding speed.
4. Microstructural analysis showed elongated grains in the base metal, refined into equiaxed grains in the weld nugget. The TMAZ contained plastically deformed grains, while the HAZ preserved the base metal structure with limited grain coarsening.
5. TEM observations confirmed dissolution and coarsening of precipitates in weld nugget, with DS-FSW promoting higher precipitate retention compared with SS-FSW, thereby contributing to improved wear behaviour.

AUTHORS' CONTRIBUTIONS

V. Kiran Kumar performed double side friction stir welding trials, conducted wear tests, examined weld microstructures and critically analysed the experimental results. K. V. Durga Rajesh supervised the project. S. R. Koteswara Rao supervised the project, devised the main conceptual ideas, verified analytical approaches, and provided critical feedback. P. Venkateswara Babu reviewed the literature and collected data on wear properties. T. Srinivasa Rao supervised the findings of this work, and wrote the manuscript with input from all authors. All authors approved the final version of the manuscript.

REFERENCES

1. W. M. Thomas, E. D. Nicholas, J. C. Needham, M. G. Church, P. Temple-Smith, and C. J. Dawes (G.B. Patent Application No. 9125978.8: December 1991).
2. R. S. Mishra and Z. Y. Ma, *Mater. Sci. Eng. R*, **50**, Iss. 1–2: 1 (2005).
3. G. Cam and S. Mistikoglu, *J. Mater. Eng. Perform.*, **23**, No. 6: 1936 (2014).
4. R. Rai, A. De, H. K. D. H. Bhadeshia, and T. DebRoy, *Sci. Technol. Weld. Joining*, **16**, Iss. 4: 325 (2011).
5. A. Arora, A. De, and T. DebRoy, *Scr. Mater.*, **64**: 9 (2011).
6. M. Mehta, A. Arora, A. De, and T. DebRoy, *Metall. Mater. Trans. A*, **42A**, No. 9: 2716 (2011).
7. A. Arora, M. Mehta, A. De, and T. DebRoy, *Int. J. Adv. Manuf. Technol.*, **61**: 911 (2012).
8. M. Mehta, A. De, and T. DebRoy, *Sci. Technol. Weld. Joining*, **19**, No. 6: 534 (2014).
9. X. He, F. Gu, and A. Ball, *Prog. Mater. Sci.*, **65**: 1 (2014).
10. Z. Y. Ma, A. H. Feng, D. L. Chen, and J. Shen, *Crit. Rev. Solid State Mater. Sci.*, **43**, Iss. 1: 269 (2018).
11. A. K. Srivastava, A. Nag, S. Dwivedi, A. R. Dixit, and S. Hloch, *Int. J. Adv. Manuf. Technol.*, **127**, Iss. 3–4: 1243 (2023).
12. A. K. Srivastava, N. Kumar, A. Saxena, and S. Tiwari, *Int. J. Cast Met. Res.*, **34**, Iss. 6: 169 (2021).
13. A. K. Srivastava, A. R. Dixit, M. Maurya, A. Saxena, N. K. Maurya, S. P. Dwivedi, and R. Bajaj, *Mater. Chem. Phys.*, **266**: 124572 (2021).
14. A. K. Srivastava, N. Kumar, and A. R. Dixit, *Mater. Sci. Eng. B*, **263**: 114832 (2021).
15. R. Kumar, K. Singh, and S. Pandey, *Trans. Nonferrous Met. Soc. China*, **22**, Iss. 2: 288 (2012).
16. P. Vincent, J. Alexis, E. Andrieu, J. Delfosse, M. C. Lafont, and C. Blanc, *Corros. Sci.*, **73**: 130 (2013).
17. T. Srinivasa Rao, G. Madhusudhan Reddy, and S. R. Koteswara Rao, *Trans. Nonferrous. Met. Soc. China*, **25**, No. 6: 1170 (2015).
18. T. Srinivasa Rao, S. R. Koteswara Rao, and G. Madhusudhan Reddy, *Materialwiss. Werkstofftech.*, **49**: 851 (2018).
19. T. Srinivasa Rao, M. Selvaraj, S. R. Koteswara Rao, and T. Ramakrishna, *Materialwiss. Werkstofftech.*, **52**: 308 (2021).
20. I. Hejazi, S.E. Mirsalehi, *Trans. Nonferrous Met. Soc. China*, **26**, Iss. 3: 676 (2016).
21. W. F. Xu, W. Zhang, and X. L. Wu, *Metall. Mater. Trans. A*, **48**: 1078 (2017).
22. M. R. Zhou, Y. Morisada, H. Fujii, and T. Ishikawa, *J. Mater. Process. Technol.*, **254**: 91 (2018).
23. V. Kiran Kumar, K. V. Durga Rajesh, S. R. Koteswara Rao, T. Ramakrishna, and T. Srinivasa Rao, *Metall. Res. Technol.*, **121**, No. 107: 1 (2024).
24. X. Zhou, Z. Li, J. Wang, and Y. Chen, *Wear*, **526**: 204993 (2023).
25. Y. Li, H. Wu, and B. Sun, *Mater. Today Commun.*, **26**: 102016 (2021).
26. A. Suresh, S. Natarajan, and R. Rathi, *Procedia Struct. Integr.*, **45**: 166 (2023).
27. J. A. Wert, *Scr. Mater.*, **15**, No. 4: 445 (1981).
28. G. W. Lorimer, *Precipitation Processes in Solids* (Eds. K. C. Russell and H. I. Aaronson) (Warrendale, PA: 1978).